Inorganic Chemistry

Article

pubs.acs.org/IC

Pentanuclear 3d−4f Heterometal Complexes of $M^{II}_3Ln^{III}_2$ (M = Ni, Cu, Zn and Ln = Nd, Gd, Tb) Combinations: Syntheses, Structures, Magnetism, and Photoluminescence Properties

Manoranjan Maity,[†] Mithun Chandra Majee,[†] Sanchita Kundu,[†] Swarna Kamal Samanta,[‡] E. Carolina Sañudo,[§] Sanjib Ghosh,[‡] and Muktimoy Chaudhury*[,†]

[†]Department of Inorganic Chemistry, Indian Association for the Cultivation of Science, Kolkata 700 032, India

[‡]Department of Chemistry, Presidency University, 86/1 College Street, Kolkata 700 073, India

[§]Departament de Quimica Inorgànica i Institut de Nanociència i Nanotecnologia, Universitat de Barcelona, Diagonal 645, 08028 Barcelona, Spain

Supporting Information

ABSTRACT: A new family of pentanuclear 3d−4f heterometal complexes of general composition $[Ln^{III}_2(M^{II}L)_3(\mu_3\text{-}O)_3H](ClO_4)\cdot xH_2O$ (**1**−**5**) [Ln = Nd, M = Zn, **1**; Nd, Ni, **2**; Nd, Cu, **3**; Gd, Cu, **4**; Tb, Cu, **5**] have been synthesized in moderate yields (50−60%) following a self-assembly reaction involving the hexadentate phenol-based ligand, viz., *N*,*N*-bis(2-hydroxy-3-methoxy-5-methylbenzyl)-*N*′,*N*′-diethylethylenediamine (H_2L). Single-crystal X-ray diffraction analyses have been used to characterize these complexes. The compounds are all isostructural, having a 3-fold axis of symmetry that passes through the 4f metal centers. The $[M^{II}L]$ units in these complexes are acting as bis-bidentate metalloligands and, together with μ_3-oxido bridging ligands, complete the slightly distorted monocapped square antiprismatic nine-coordination environment around the 4f metal centers. The cationic complexes also contain a H^+ ion that occupies the central position at the 3-fold axis. Magnetic properties of the copper(II) complexes (**3**−**5**) show a changeover from antiferromagnetic in **3** to ferromagnetic 3d−4f interactions in **4** and **5**. For the isotropic Cu^{II}−Gd^{III} compound **4**, the simulation of magnetic data provides very weak Cu−Gd (J_1 = 0.57 cm^{-1}) and Gd−Gd exchange constants (J_2 = 0.14 cm^{-1}). Compound **4** is the only member of this triad, showing a tail of an out-of-phase signal in the ac susceptibility measurement. A large-spin ground state (S = 17/2) and a negative value of D (−0.12 cm^{-1}) result in a very small barrier (8 cm^{-1}) for this compound. Among the three $Nd^{III}_2M^{II}_3$ (M = Zn^{II}, Ni^{II}, and Cu^{II}) complexes, only the Zn^{II} analogue (**1**) displays an NIR luminescence due to the $^4F_{3/2} \rightarrow {}^4I_{11/2}$ transition in Nd^{III} when excited at 290 nm. The rest of the compounds do not show such Nd^{III}/Tb^{III}-based emission. The paramagnetic Cu^{II} and Ni^{II} ions quench the fluorescence in **2**−**5** and thereby lower the population of the triplet state.

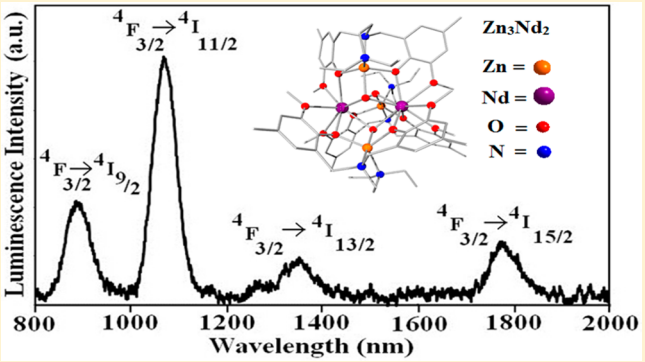

INTRODUCTION

Heterometal complexes containing 3d−4f metal ion combinations are an area of intensive research in recent times,[1,2] primarily because of their interesting magnetic and photophysical properties. Almost all lanthanum(III) complexes exhibit substantial intrinsic magnetic anisotropy, leading to large magnetic moments in the ground state. Researchers have tried to exploit these large-spin ground states (S_T), especially those of Gd^{III}, Tb^{III}, Dy^{III}, Ho^{III}, etc., to synthesize complexes that could eventually behave as single-molecule magnets (SMMs)[3] or act as low-temperature molecular magnetic coolers (MMCs).[4] The initial interest in this area stems from a classic paper by Gatteschi et al. that describes ferromagnetic interactions between copper(II) and isotropic gadolinium(III) ions in a discrete trinuclear complex.[5] A large number of 3d−4f complexes have since been reported.[6,7] Many of these find possible applications, albeit at very low temperatures, in the areas of information storage, molecular spintronics, and quantum computation.[8]

There is a growing interest also in the coordination complexes of Eu^{III} and Tb^{III} ions because of their intense, long-lived, and line-like emissions in the visible region, leading to their widespread applications as display devices, luminescent sensors, and probes for clinical use.[9] In contrast, there are some other lanthanides also, viz., Nd^{III}, Yb^{III}, and Er^{III}, showing luminescence in the near-infrared (NIR) region,[10] which has been only scantily investigated up until now and emerges lately as a field of priority research, leading to the development of many application materials for optical and medical uses.[10]

Received: May 20, 2015
Published: September 25, 2015

DOI: 10.1021/acs.inorgchem.5b01142
Inorg. Chem. 2015, 54, 9715−9726

Scheme 1. Protocol for the Synthesis of Complexes 1−5

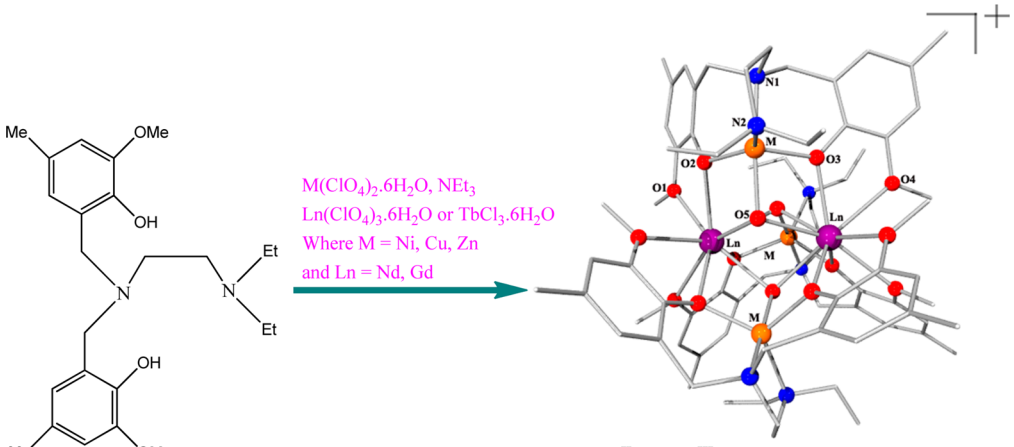

Generally, the 4f−4f transitions in lanthanides are Laporte-forbidden, which makes direct excitation of their excited states inefficient, resulting in very low absorption coefficients. To circumvent this problem, often a coordinated organic ligand that strongly absorbs in the UV region can be used effectively for fast energy transfer from the ligand-based triplet state to the lanthanide. This is the usual way of achieving sensitized emission (the so-called antenna effect[11]) in the visible region from Eu^{III}- and Tb^{III}-based compounds.[12] However, for NIR-emissive lanthanide ions with lower energy luminescent levels, the use of UV light to perform excitation is energetically an inefficient process. In such cases use of 3d−4f hybrid compounds having LMCT states as the energy donors for sensitizing Ln(III) emission offers numerous advantages.[10g,13] Quite a good number of 3d−4f compounds have since been prepared to study their luminescence behavior in the NIR region.[10]

For quite some time, we have had an ongoing program on the coordination chemistry of 3d−4f hybrid complexes.[14−16] Considering that organic ligands play a central role in the successful synthesis of polymetal complexes, we have used bis-phenolate ligands on those previous occasions[14−16] for the successful synthesis of many 3d−4f complexes in which the bridging phenolate moiety plays a dominant role. The present work is a natural extension of that program where we introduced a new hexadentate ligand, viz., *N*,*N*-bis(2-hydroxy-3-methoxy-5-methylbenzyl)-*N*′,*N*′-diethylethylenediamine (H_2L) involving methoxy substitution at the 3-position of the phenol moiety, as shown in Scheme 1. Such molecules can act as compartmental ligands, providing two pockets of differential occupancy for the efficient binding of 3d−4f heterometal centers as reported in the literature.[17] In fact, the $-OCH_3$ group placed in *ortho* position with respect to a phenolate donor can generate optimum space for the preferential binding of larger 4f metal ions.[17]

Herein, we report the syntheses and X-ray structures of a new family of isostructural $Ln^{III}_2M^{II}_3$-type pentanuclear complexes of molecular formula $[Ln^{III}_2(M^{II}L)_3(\mu_3\text{-}O)_3H]\text{-}(ClO_4)\cdot xH_2O$ (**1**−**5**) (where M^{II} = Ni, Cu, Zn, and Ln^{III} = Nd, Gd, Tb) (Scheme 1) using the ligand H_2L that fits our strategy. The compounds have been prepared for comparison studies in order to check how the individual metal ions (both 3d and 4f types) influence the magnetic and photophysical properties of the combined system. The photophysical properties of compounds **1**−**5** and the magnetic properties of the $Cu^{II}_3Nd^{III}_2$ (**3**), $Cu^{II}_3Gd^{III}_2$ (**4**), and $Cu^{II}_3Tb^{II}_2$ (**5**) combinations have been explored in greater detail for a comparative study. The results clearly indicate that a careful choice of transition metal and lanthanide ion in the combination is important to get the desired magnetic and photophysical properties.

EXPERIMENTAL SECTION

Materials. 2-Methoxy-4-methylphenol and *N*,*N*-diethylethylenediamine were obtained from Sigma-Aldrich. Solvents were reagent grade, dried using appropriate reagents,[18] and distilled under nitrogen prior to their use. All other chemicals were reagent grade, available commercially, and used as received.

Synthesis of Ligand. To a solution of *N*,*N*-diethylethylenediamine (1.16 g, 10 mmol) in methanol (30 mL) was added paraformaldehyde (0.6 g, 20 mmol) as a solid under stirring. The mixture was refluxed for 2 h to get a clear solution. It was cooled to room temperature. To this solution was added 2-methoxy-4-methyl phenol (2.76 g, 20 mmol) as a solid. The resulting mixture was further refluxed for 12 h and cooled to room temperature. The solution was rotary-evaporated to near dryness to get an off-white solid, which was recrystallized from acetonitrile to get a white crystalline product. Yield: 3.61 g (80%); mp 90 °C. Anal. Calcd for $C_{24}H_{36}N_2O_4$: C, 69.20; H, 8.71; N, 6.73. Found: C, 69.80; H, 8.58; N, 6.90. IR (KBr disk, cm^{-1}): 2970, 2833, 1496, 1380, 1298, 1242, 1151, 1072, 835, 777. ^{1}H NMR (500 MHz, $CDCl_3$, δ/ppm): 1.01 (t, J = 9.0 Hz, 6H, $-CH_3$), 2.23 (s, 6H, CH_3), 2.51 (q, J = 9.0 Hz, 4H, $-CH_2-$), 2.61 (m, 4H, $N-CH_2-CH_2-N$), 3.60 (s, 4H, benzylic), 3.82 (s, 6H, $-OCH_3$), 6.48 (s, 2H, aryl), 6.59 (s, 2H, aryl). UV−vis (CH_2Cl_2) [λ_{max}/nm (ε/mol^{-1} cm^2)]: 226 (3500), 285 (6050). ESI-MS (in CH_3CN): m/z 417.52 ($M + H^+$).

Preparation of Complexes. ***Safety Note! Caution!*** *Perchlorate salts of metal complexes are potentially explosive and should be handled only in small quantities with sufficient care.*[19]

*$[Nd_2(ZnL)_3(\mu_3\text{-}O)_3H](ClO_4)\cdot xH_2O$ (**1**).* To a solution of H_2L (0.104 g, 0.25 mmol) in methanol (30 mL) was added as a solid $Zn(ClO_4)_2\cdot 6H_2O$ (0.180 g, 0.50 mmol), followed by triethylamine (0.051 g, 0.5

DOI: 10.1021/acs.inorgchem.5b01142
Inorg. Chem. 2015, 54, 9715−9726

Table 1. Summary of the Crystallographic Data for the Complexes 1−5

parameter	1	2	3	4	5
composition	$C_{72}H_{102}ClN_6Nd_2Zn_3O_{19}$	$C_{72}H_{102}ClN_6Nd_2Ni_3O_{19}$	$C_{72}H_{102}ClN_6Nd_2Cu_3O_{19}$	$C_{72}H_{102}ClN_6Gd_2Cu_3O_{19}$	$C_{72}H_{102}ClN_6Tb_2Cu_3O_{19}$
fw	1875.63	855.65	1870.14	1896.16	1899.50
cryst syst	cubic	cubic	cubic	cubic	cubic
space group	$P\bar{4}_3n$	$P\bar{4}_3n$	$P\bar{4}_3n$	$P\bar{4}_3n$	$P\bar{4}_3n$
a, Å	26.0320(5)	25.9721(4)	25.9355(7)	26.1090(7)	26.0903(4)
V, Å^3	17641.0(10)	17519.5(8)	17445.5(14)	17798.0(14)	17759.8(8)
ρ_{calc}, Mg m^{-3}	1.412	1.407	1.424	1.415	1.421
temp, K	150(2)	150(2)	150(2)	150(2)	150(2)
λ (Mo K$_\alpha$), Å	0.710 73	0.710 73	0.710 73	0.710 73	0.710 73
Z	8	8	8	8	8
$F(000)/\mu$ mm^{-1}	7640/2.054	7592/1.891	7616/1.983	7680/2.267	7696/2.371
$2\theta_{max}$, deg	53.68	48.84	46.08	48.82	46.74
reflns collected/ unique	18 1578/6325	15 7230/4830	105 189/3927	79 432/4904	141 584/4324
R_{int}/GOF on F^2	0.0631/3.188	0.1322/1.045	0.1322/1.663	0.0751/1.049	0.0910/1.062
no. of params	317	316	318	316	316
R_1[a](F_o), wR_2[b](F_o) (all data)	0.0383, 0.0824	0.0505, 0.1370	0.0758, 0.2054	0.0580, 0.1552	0.0470, 0.1332
largest diff peak, deepest hole, e Å^{-3}	0.881, 0.417	0.809, −0.497	1.342, −0.835	1.005, −0.520	0.527, −0.300

[a] $R = \sum||F_o| - |F_c||/\sum|F_o|$. [b] $wR = [\sum[w((F_o^2 - F_c^2)^2]/\sum w(F_o^2)^2]^{1/2}$.

mmol) and $Nd(ClO_4)_3{\cdot}6H_2O$ (0.14 g, 0.25 mmol). The resulting solution was stirred for an hour and then filtered. The filtrate was kept in the open air for slow evaporation. A white crystalline compound was obtained within 2−3 days. Some of these block-shaped crystals were of X-ray diffraction quality and used directly for crystal structure analysis. The compound is prone to solvent loss. Drying under vacuum for a long time afforded a fully desolvated sample, used for various measurements including microanalysis. Yield: 0.25 g (60%). Anal. Calcd for $C_{72}H_{103}ClN_6O_{19}Nd_2Zn_3$: C 46.08, H 5.53, N 4.48. Found: C 46.13, H 5.49, N 4.47. FT-IR bands (KBr pellet, cm^{-1}): 3431b, 2921w, 1490s, 1382m, 1325m, 1255s, 1153m, 1091b, 817m, 624m.

$[Nd_2(NiL)_3(\mu_3\text{-}O)_3H](ClO_4)\cdot xH_2O$ (**2**). To a methanol solution (30 mL) of H_2L (0.10 g, 0.25 mmol) was added as a solid $Ni(ClO_4)_2{\cdot}6H_2O$ (0.18 g, 0.5 mmol). To this green solution was added triethylamine (0.05 g, 0.5 mmol) followed by $Nd(ClO_4)_3{\cdot}6H_2O$ (0.14 g, 0.25 mmol). The resulting mixture was refluxed for an hour. The solution was cooled to room temperature and filtered. The filtrate was left in the open air for slow evaporation. A green crystalline compound was obtained within 2−3 days. Some of these block-shaped crystals were of diffraction quality and used directly for X-ray crystal structure analysis. The compound is prone to solvent loss. Drying under vacuum for a long time afforded a fully desolvated sample, used for various measurements including microanalysis. Yield: 0.21 g (50%). Anal. Calcd for $C_{72}H_{103}ClN_6O_{19}Nd_2Ni_3$: C 46.58, H 5.59, N 4.53. Found: C 46.32, H 5.62, N 4.47. FT-IR bands (KBr pellet, cm^{-1}): 3429b, 2920w, 1492s, 1381m, 1327m, 1259s, 1155m, 1089b, 819m, 624m.

$[Nd_2(CuL)_3(\mu_3\text{-}O)_3H](ClO_4)\cdot xH_2O$ (**3**). This compound was prepared following a similar procedure to that described above for compound **2** using $Cu(ClO_4)_2{\cdot}6H_2O$ (0.18 g, 0.5 mmol) instead of $Ni(ClO_4)_2{\cdot}6H_2O$. A brown crystalline compound was obtained within 2−3 days. Some of these block-shaped crystals were of diffraction quality and used directly for X-ray crystal structure analysis. The compound is prone to solvent loss. Drying under vacuum for a long time afforded a fully desolvated sample, used for various measurements including microanalysis. Yield: 0.23 g (55%). Anal. Calcd for $C_{72}H_{103}ClN_6O_{19}Cu_3Nd_2$: C 46.22, H 5.55, N 4.49. Found: C 45.97, H 5.62, N 4.54. FT-IR bands (KBr pellet, cm^{-1}): 3433b, 2920w, 1492s, 1381m, 1330m, 1259s, 1155s, 1076b, 823m, 623m.

$[Gd_2(CuL)_3(\mu_3\text{-}O)_3H](ClO_4)\cdot xH_2O$ (**4**). This compound was prepared following a similar procedure to that described above for **3** using $Gd(ClO_4)_3{\cdot}6H_2O$ (0.14 g, 0.25 mmol) instead of $Nd(ClO_4)_3{\cdot}6H_2O$. The compound is prone to solvent loss. Drying under vacuum for a long time afforded a fully desolvated sample, used for various measurements including microanalysis. Yield: 0.26 g (60%). Anal. Calcd for $C_{72}H_{103}ClN_6O_{19}Cu_3Gd_2$: C 45.58, H 5.47, N 4.43. Found: C 45.49, H 5.43, N 4.38. FT-IR bands (KBr pellet, cm^{-1}): 3433b, 2918w, 1494s, 1380w, 1330m, 1261s, 1153m, 1089b, 823m, 624m.

$[Tb_2(CuL)_3(\mu_3\text{-}O)_3H](ClO_4)\cdot xH_2O$ (**5**). This compound was prepared following a similar procedure to that described above for **3** using $TbCl_3{\cdot}6H_2O$ (0.083 g, 0.25 mmol) instead of $Nd(ClO_4)_3{\cdot}6H_2O$. The compound is prone to solvent loss. Drying under vacuum for a long time afforded a fully desolvated sample, used for various measurements including microanalysis. Yield: 0.26 g (60%). Anal. Calcd for $C_{72}H_{103}ClN_6O_{19}Cu_3Tb_2$: C 45.50, H 5.46, N 4.42. Found: C 45.38, H 5.51, N 4.39. FT-IR bands (KBr pellet, cm^{-1}): 3433b, 2918w, 1494s, 1382s, 1330m, 1261s, 1155m, 1074b, 825m, 624m.

Physical Measurements. IR spectroscopic measurements were made on samples pressed into KBr pellets using a Shimadzu 8400S FT-IR spectrometer, while for UV−visible spectral measurements, a PerkinElmer Lambda 950 UV/vis/NIR and a Hitachi 4010 spectrophotometer were employed. Elemental analyses (for C, H, and N) were performed at IACS on a PerkinElmer model 2400 Series II CHN analyzer. Magnetic measurements were carried out on polycrystalline samples (about 30 mg) at the Unitat de Mesures Magnètiques of the Universitat de Barcelona (Spain) with a Quantum Design SQUID MPMS-XL magnetometer equipped with a 5 T magnet. Diamagnetic corrections were calculated using Pascal's constants, and an experimental correction for the sample holder was applied.

X-ray Crystallography. Suitable crystals of **1** (white block 0.20 × 0.25 × 0.15 mm^3), **2** (green block 0.15 × 0.25 × 0.30 mm^3), **3** (brown block 0.25 × 0.15 × 0.20 mm^3), **4** (brown block 0.20 × 0.25 × 0.30 mm^3), and **5** (dark brown block 0.25 × 0.20 × 0.30 mm^3) were coated with perfluoropolyether oil before mounting. Intensity data for the aligned crystals of all the complexes were recorded at 150(2) K employing a Bruker SMART APEX II CCD diffractometer equipped with a monochromatized Mo Kα radiation (λ = 0.710 73 Å) source. No crystal decay was observed during the data collections. In all cases, absorption corrections based on multiscans using the SADABS software[20] were applied. The structures were solved by direct methods[21] and refined on F^2 by a full-matrix least-squares procedure based on all data minimizing $wR = [\sum[w(F_o^2 - F_c^2)^2]/\sum(F_o^2)^2]^{1/2}$, $R = \sum||F_o| - |F_c||/\sum|F_o|$ and $S = [\sum[w(F_0^2 - F_c^2)^2]/(n - p)]^{1/2}$. SHELXL-2013 was used for both structure solutions and refinements.[22] A summary of the relevant crystallographic data and the final refinement details are given in Table 1. All non-hydrogen atoms were

DOI: 10.1021/acs.inorgchem.5b01142
Inorg. Chem. 2015, 54, 9715−9726

refined anisotropically. The positions of hydrogen atoms were calculated and isotropically fixed in the final refinement [d(C−H) = 0.95 Å, with the isotropic thermal parameter of U_{iso}(H) = 1.2 U_{iso}(C)]. The SMART and SAINT software packages[23] were used for data collection and reduction, respectively. Crystallographic diagrams were drawn using the DIAMOND software package.[24] There is a unique H^+ ion in these cationic complexes. We failed to identify crystallographically the exact position of that hydrogen ion. Also severely disordered water molecules in **1**−**5** were removed by SQUEEZE during the structural refinements. In addition, the structures also contain solvent-accessible voids, which were smoothened using the PLATON/SQUEEZE routine.

Photoluminescent Measurements. The steady-state emission measurements were carried out using a Hitachi model F-7000 spectrofluorimeter equipped with a 150 W xenon lamp at 298 K using a stoppered cell of 1 cm path length. The relative fluorescence quantum yield of ligand emission at 298 K was determined in each case using the following relations:

$$\phi_M/\phi_L = (I_M \times OD_L)/(I_L \times OD_M) \quad (1)$$

where M is any of the compounds **1**−**5** and L is the free ligand. I_M and I_L are the intensities of total fluorescence spectra obtained from considering the total area under the emission curve. Emission studies at 77 K were made using a Dewar system having a 5 mm o.d. quartz tube. The freezing of the sample at 77 K was done at the same rate for all the samples. Phosphorescence spectra were recorded on a Hitachi model F-7000 spectrofluorimeter equipped with phosphorescence accessories at 77 K and also in a QM-30 fluorimeter from PTI, USA, equipped with a xenon flash lamp of repetition rate 150 Hz with a gated detection system having start and end window times of 150 and 1500 μs, respectively. The lifetime of the singlet state was measured using TCSPC from PTI, USA, using the subnanosecond pulsed LED source (290 nm having a pulse width of 600 ps [full width at half-maximum]) from PicoQuant, Germany, operating at a high repetition rate of 10 MHz driven by a PDL 800-B driver, also from PicoQuant, Germany. Lamp profiles were measured with a band-pass of 3 nm using Ludox as the scatterer. The decay parameters were recovered using a nonlinear iterative fitting procedure based on the Marquardt algorithm.[25] The deconvolution technique used can determine the lifetime up to 150−200 ps. The quality of fit has been assessed over the entire decay, including the rising edge, and tested with a plot of weighted residuals and other statistical parameters, e.g., the reduced χ^2 ratio.[26] The decay times in the milliseconds or longer range were measured by phosphorescence time based acquisition mode of the QM-30 fluorimeter in which emission intensity is measured as a function of time. The decay parameters were recovered using a nonlinear iterative fitting procedure based on the Marquardt algorithm.[27]

RESULTS AND DISCUSSION

Synthesis. The heterometallic pentanuclear complexes $[Nd_2(ML)_3(\mu_3\text{-}O)_3H](ClO_4)\cdot xH_2O$ (M = Zn **1**; Ni **2**; Cu **3**) and $[Ln_2(CuL)_3(\mu_3\text{-}O)_3H](ClO_4)\cdot xH_2O$ (Ln = Gd **4**; Tb **5**) have been synthesized as crystalline solids in moderate yields (50−60%) by a single-step self-assembly reaction. In actual procedure, $M^{II}(ClO_4)_2$, H_2L, and $Ln^{III}(ClO_4)_3$ ($TbCl_3$ for **5**) were mixed together in 2:1:1 molar proportion in methanol solvent as summarized in Scheme 1. For compound **1**, stirring of this solution at room temperature for an hour and subsequent workup are needed to get the compound in the crystalline form. For the remaining compounds **2**−**5**, however, reactions under refluxing condition are followed in order to avoid long hours of stirring. For compound **1**, reaction under refluxing condition generates powdered compound, possibly because of its lower solubility in common organic solvents. Perchlorate as counteranion balances the charge of these cationic complexes. The μ_3-oxido bridges in the core of the complexes (as established by X-ray crystallography, see later) are possibly generated in the reaction medium from the residual water in the solvent. High thermodynamic stability of this self-assembled product uses each of these μ_3-oxido groups to bind the individual 3d metal ion to both the lanthanide centers. The phenolic−OH groups in the coordinated ligands are all deprotonated and also act as a bridge between the two neighboring 3d and 4f heterometal centers. The presence of a perchlorate anion requires that the cationic part of the molecule should have, for the sake of charge balance, a hydrogen ion, which we could not locate crystallographically in the molecule. However, a central position has been assigned for this hydrogen atom considering the symmetry of the molecule as revealed from X-ray crystallography (see later).

The IR spectra of the complexes (**1**−**5**) show all the characteristic bands for the coordinated pentadentate ligand $[L]^{2-}$. One such band is the prominent one due to ν(C−O/phenolate) stretching appearing at ca. 1255 cm^{-1}. Appearance of a strong signature band in the 1490−1494 cm^{-1} range is due to the −OMe group of the ligand. The presence of a strong band in the 1075−1090 cm^{-1} range together with a weak bending vibration at 620 cm^{-1} is the fingerprint of ionic perchlorate present in these compounds.[28]

Description of Crystal Structures. All the reported compounds are isostructural; they crystallized in the cubic space group $P\bar{4}_3n$ with eight molecular mass units accommodated per cell. A perspective view of the molecular structure of **3** is displayed in Figure 1. The views of the molecular

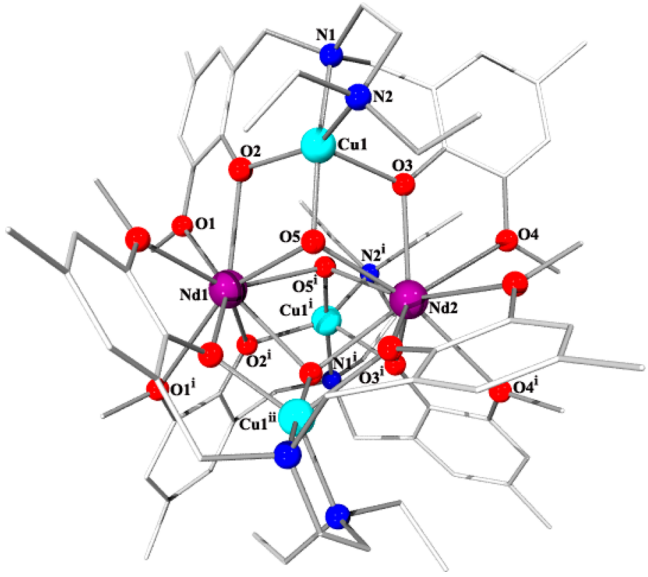

Figure 1. Partially labeled POV-Ray (in ball-and-stick form) diagram showing the atom-labeling scheme in the cationic part of complex **3**.

structures of the remaining compounds **1**, **2**, **4**, and **5** (Figures S1−S4) are available in the Supporting Information. Identical atom-labeling schemes have been adopted for all of these closely similar structures for easy comparison of their relevant metrical parameters (Table 2). For the sake of brevity, only a generic description of the crystal structure of **3** as a prototype is given here. The molecule has a 3-fold axis of symmetry that passes through the neodymium metal centers and generates three asymmetric units, each having a Cu and two Nd metal centers, one fully deprotonated ligand $[L]^{2-}$, and a μ_3-oxido atom (Figure 2). The copper center Cu1 is five-coordinated

DOI: 10.1021/acs.inorgchem.5b01142
Inorg. Chem. 2015, 54, 9715−9726

Table 2. Selected Bond Distances and Angles for 1−5[a]

parameter	1; M = Zn; Ln = Nd	2; M = Ni; Ln = Nd	3; M = Cu; Ln = Nd	4; M = Cu; Ln = Gd	5; M = Cu; Ln = Tb
			Bond Distances (Å)		
Ln1—O1	2.633(5)	2.595(8)	2.602(11)	2.687(9)	2.566(9)
Ln1—O2	2.425(5)	2.481(7)	2.479(11)	2.325(10)	2.385(9)
Ln1—O5	2.466(5)	2.440(7)	2.470(11)	2.479(10)	2.385(8)
Ln2—O3	2.506(5)	2.428(7)	2.375(13)	2.419(10)	2.315(10)
Ln2—O4	2.578(5)	2.702(7)	2.723(10)	2.561(10)	2.682(8)
Ln2—O5	2.427(4)	2.459(7)	2.500(12)	2.399(9)	2.464(9)
M1—O2	2.065(4)	2.018(7)	2.007(12)	2.172(10)	2.002(8)
M1—O3	2.016(5)	2.021(7)	2.203(11)	2.000(1)	2.165(8)
M1—O5	2.031(4)	2.003(6)	1.945(10)	1.938(9)	1.942(8)
M1—N1	2.100(6)	2.038(9)	2.007(12)	2.003(12)	2.019(11)
M1—N2	2.107(6)	2.089(9)	2.057(13)	2.058(15)	2.079(11)
			Bond Angles (deg)		
$O5^{i}$—Ln1—O5	68.93(16)	69.8(3)	70.1(4)	69.2(3)	71.9(3)
O5—Ln1—$O2^{i}$	125.01(15)	128.6(2)	128.4(4)	126.0(3)	131.1(3)
$O5^{i}$—Ln1—O2	66.17(15)	73.5(2)	73.5(3)	67.6(3)	74.9(3)
O5—Ln1—O2	66.41(14)	64.3(2)	63.7(4)	66.2(3)	64.2(3)
O5—Ln1—$O1^{i}$	153.36(15)	143.4(3)	143.2(4)	156.1(3)	147.5(3)
$O5^{i}$—Ln1—O1	96.48(15)	83.4(3)	82.3(4)	98.7(3)	88.0(3)
O5—Ln1—O1	128.03(14)	124.2(2)	123.1(3)	127.2(3)	126.6(3)
$O2^{i}$—Ln1—O2	118.99(4)	119.83(2)	119.78(4)	119.24(7)	119.967(12)
$O2^{i}$—Ln1—O1	87.75(15)	72.6(3)	72.6(4)	88.8(4)	73.4(3)
O2—Ln1—O1	62.15(14)	61.4(2)	61.0(4)	62.0(3)	62.9(3)
O2—Ln1—$O1^{i}$	136.28(15)	147.9(3)	149.2(4)	133.3(3)	140.9(3)
O1—Ln1—$O1^{i}$	74.57(17)	92.1(3)	93.6(4)	71.6(4)	83.8(3)
$O3^{i}$—Ln2—O3	119.951(8)	119.05(6)	118.99(1)	119.964(14)	119.29(7)
O3—Ln2—O4	61.12(15)	61.6(2)	61.5(4)	62.6(3)	62.4(3)
O3—Ln2—$O4^{i}$	143.32(15)	133.7(2)	134.3(4)	141.2(3)	133.6(3)
$O3^{i}$—Ln2—O4	73.77(16)	90.0(2)	90.0(4)	73.6(4)	87.7(3)
O3—Ln2—$O5^{i}$	75.10(15)	67.7(2)	66.5(4)	75.0(3)	67.5(3)
$O3^{i}$—Ln2—O5	129.78(15)	125.3(2)	125.1(4)	131.0(3)	126.1(3)
$O4^{i}$—Ln2—O4	87.39(15)	72.2(3)	72.9(4)	84.2(3)	71.7(3)
O3—Ln2—O5	64.43(15)	65.1(2)	66.0(3)	64.0(3)	66.5(3)
$O5^{i}$—Ln2—O5	70.20(17)	69.2(3)	69.2(4)	71.9(4)	69.2(3)
O5—Ln2—$O4^{i}$	147.10(16)	157.5(2)	156.1(3)	147.8(3)	155.0(3)
$O5^{i}$—Ln2—O4	86.85(15)	98.8(2)	98.0(4)	87.8(3)	98.4(3)
O5—Ln2—O4	124.63(15)	125.7(2)	126.5(3)	126.0(3)	128.1(3)
O5—M1—O2	81.78(18)	81.3(3)	82.8(5)	79.2(4)	79.9(4)
O5—M1—O3	81.09(19)	81.6(3)	79.4(5)	80.8(4)	79.2(4)
O2—M1—O3	113.08(19)	112.4(3)	107.4(4)	102.9(4)	108.8(3)
O5—M1—N1	171.9(2)	174.0(3)	170.2(5)	170.0(5)	169.9(4)
O2—M1—N1	92.0(2)	94.7(3)	95.9(5)	92.8(4)	96.8(4)
O3—M1—N1	96.7(2)	95.9(3)	91.8(5)	96.4(4)	93.0(4)
O5—M1—N2	101.6(2)	100.5(3)	100.7(5)	101.3(5)	101.3(4)
O2—M1—N2	115.6(2)	144.9(3)	147.6(5)	108.3(5)	141.6(4)
O3—M1—N2	131.1(2)	102.5(3)	104.8(5)	142.1(5)	109.1(4)
N1—M1—N2	85.8(2)	85.4(4)	85.6(6)	86.8(6)	87.2(5)
M1—O2—Ln1	106.03(18)	105.5(3)	105.3(5)	106.2(4)	106.3(4)
M1—O5—Ln1	105.70(18)	107.5(3)	107.7(5)	108.4(4)	108.4(4)
M1—O3—Ln2	104.91(19)	106.9(3)	105.2(5)	105.6(4)	106.1(4)
M1—O5—Ln2	107.29(19)	106.4(3)	109.3(4)	108.5(4)	108.2(3)
Ln1—O5—Ln2	97.6(16)	97.7(2)	97.5(4)	96.3(4)	96.4(3)

[a]Symmetry code: (i) 1−*y*, *z*, 1−*x*; (ii) 1−*z*, 1−*x*, *y*.

with a distorted square pyramidal geometry (τ = 0.38),[29] completed by the imino nitrogen atoms N1 and N2 and the phenolate oxygen donors O2 and O3, all coming from the coordinated ligand $[L]^{2-}$ (Figure 1). The fifth coordination site is completed by a μ_3-oxido ligand O5. The basal plane of this square pyramid is made up of N1, N2, O2, and O5 donor atoms, while the apical site is occupied by an O3 donor atom to complete the square pyramidal geometry. The *trans* angles O5−Cu1−N1 and O2−Cu1−N2 formed in the basal plane are 170.2(5)° and 147.6(5)°, respectively, and the latter angle is very short of linearity due to the strain imposed by the bridging phenolate donor. Other *cis* angles O3−Cu1−O2, O3−Cu1−

DOI: 10.1021/acs.inorgchem.5b01142
Inorg. Chem. 2015, 54, 9715−9726

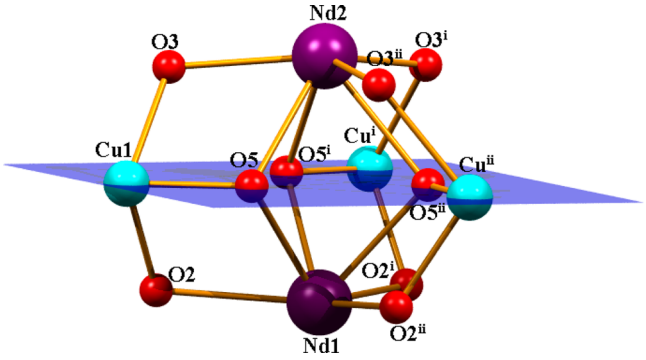

Figure 2. Skeletal view of the cationic part in **3** showing the three asymmetric units that complete the core of the molecule.

N1, O3−Cu1−N2, and O3−Cu1−O5 are 107.4(4)°, 91.8(5)°, 104.8(5)°, and 79.4(5)°, respectively, all in the expected range. The [Cu1(L)] unit, in turn, is acting as a bis-bidentate metalloligand, providing a combination of a methoxido and a bridging phenolate donor (O1, O2 and O3, O4) to bind the Nd1 and Nd2 centers. All three [Cu(L)] units behave in a similar fashion to provide six donor sites to individual Nd centers. In addition, three μ_3-oxido donors (O5) also fill up the remaining three donor sites to complete a nine-coordination environment with sufficiently distorted monocapped square antiprismatic geometry around the Nd^{III} metal centers as displayed in Figure 3 for Nd2 as the central 4f ion.

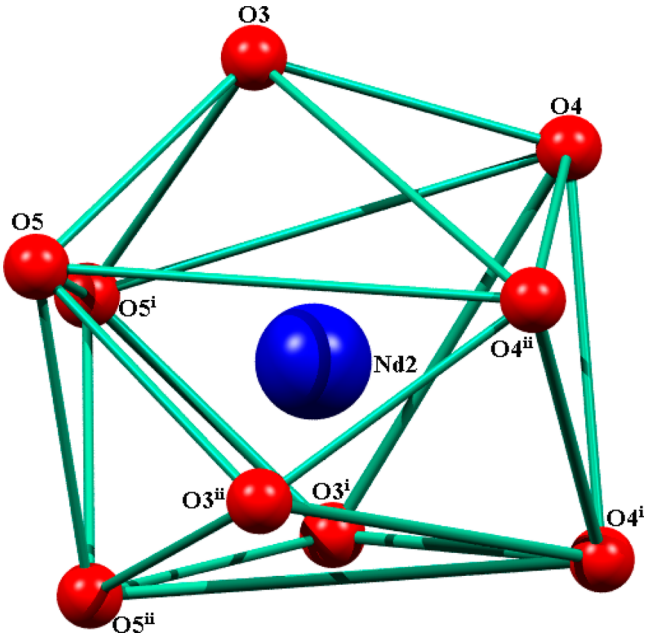

Figure 3. Monocapped square antiprismatic coordination environment around Nd2 in compound **3**.

The Nd−O bond lengths vary in the range 2.375(13) to 2.723(10) Å. The Cu1···Nd1 and Cu1···Nd2 separations are 3.577 and 3.640 Å, respectively.[30] Interestingly, the copper centers Cu1, $Cu1^{i}$, and $Cu1^{ii}$ and the μ_3-oxido atoms O5, $O5^{i}$, and $O5^{ii}$ are all lying in a common plane, while the neodymium centers Nd1 and Nd2 are lying above and below that plane on a 3-fold axis, orthogonal to the former (Figure 2). The location of the lone hydrogen ion that is believed to be present in the cationic unit is not identifiable crystallographically. Nevertheless, considering the molecule to have a 3-fold axis of symmetry with one-third of the molecule as the asymmetric unit, we believe this hydrogen atom is possibly sitting at the central point common to this plane and the 3-fold axis. The Nd1···Nd2 separation is 3.736 Å, and the Nd−O5−Nd bond angle is 97.5(4)°. Also the Cu···Cu and Cu···Nd separations are 5.34 and 3.64 Å, respectively, and the Nd−O5−Cu angles are lying in the range 107−109°.

Magnetic Studies. Magnetic data for the copper(II) complexes **3**, **4**, and **5** have been collected with the crushed polycrystalline samples. The data are shown in Figure 4 as χT vs T plots collected between 2 and 300 K at 0.3 T applied dc field. The χT product observed at 300 K for **3**, **4**, and **5** are 3.74, 17.12, and 24.74 $cm^3\ K\ mol^{-1}$, respectively, in good agreement with the expected values for three Cu(II) ions ($S = 1/2$, $C = 0.375\ cm^3\ K\ mol^{-1}$) and two lanthanide ions (Nd^{III}: $^4I_{9/2}$, $S = 3/2$, $L = 6$, $g = 8/11$ for **3**; Gd^{III}: $^8S_{7/2}$, $S = 7/2$, and $g = 2.0$ for **4**; or Tb^{III}: $^7F_6$, $S = 3$, $L = 3$, $J = 6$, and $g = 3/2$ for **5**).[31] On cooling, the χT product for compound **3** gradually decreases to $1.72\ cm^3\ K\ mol^{-1}$ at 2 K, which results most likely from the progressive thermal depopulation of the excited-state Stark sublevels due to the crystal-field effects of Nd^{3+} ions[32] and the probable weak antiferromagnetic interactions between the metal centers.[33]

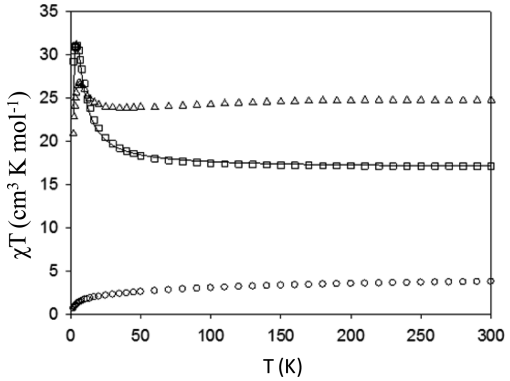

Figure 4. χT vs T plots for **3** (circles), **4** (squares), and **5** (triangles) at 0.3 T applied dc field. The solid line is the best fit to the experimental data (see text for fitting parameters).

The χT value at room temperature for **4** (17.12 $cm^3 \cdot K \cdot mol^{-1}$) is slightly higher than the expected value of 16.875 $cm^3 \cdot K \cdot mol^{-1}$. As the temperature decreases, the χT product for **4** increases slowly until a sharp increase is observed below 50 K. The observed increase is the contribution of the Cu···Gd interactions, which tend to align ferromagnetically the spins of the Gd ions at low temperature. Such ferromagnetic interactions have been reported earlier with many Cu(II)−Gd(III) compounds and are believed to be an intrinsic property of this system,[5,34,35] although antiferromagnetic interactions are also not uncommon in Cu−Gd compounds.[36] Complex **4** contains three Cu^{II} ions and two isotropic Gd^{III} ions, which have seven f-electrons but no spin−orbit coupling contribution, so the magnetic data can be modeled using the spin exchange Hamiltonian shown in eq 2 and the metal ion numbering of Scheme 2:

DOI: 10.1021/acs.inorgchem.5b01142
Inorg. Chem. 2015, 54, 9715−9726

$$H = -J2[\hat{S}Gd1.\hat{S}Gd2] - J1[\hat{S}Cu1.\hat{S}Gd1 + \hat{S}Cu1.\hat{S}Gd2 + \hat{S}Cu2.\hat{S}Gd1 + \hat{S}Cu2.\hat{S}Gd2 + \hat{S}Cu3.\hat{S}Gd1 + \hat{S}Cu3.\hat{S}Gd2] \quad (2)$$

Scheme 2. Simplified Two-Exchange Coupling Constants Model for Compound 4

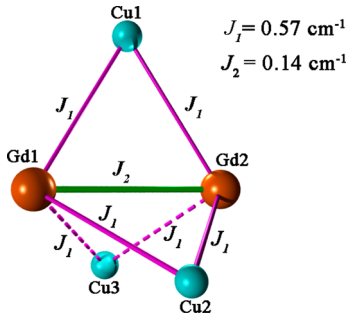

In order to solve the above isotropic spin−spin Hamiltonian exactly, a matrix of dimension 512 × 512 must be diagonalized, and this can be done satisfactorily with an available software like PHI.[37] The χT data for **4** were fitted using this software. As usual for 3d−4f complexes, the magnetic couplings are very weak. The best fitting is shown in Figure 4 as a solid line. The Cu−Gd exchange constant is J_1 = 0.57 cm^{-1} and the Gd−Gd constant J_2 is 0.14 cm^{-1}. This model predicts a spin ground state of S_T = 17/2 for **4**. The magnetization data collected at 2 K were fitted using the giant spin model for S_T = 17/2 and g = 2.00 with PHI. This allowed us to introduce the D value for the $Cu^{II}_3Gd^{III}_2$ complex **4**. The best fit is shown in Figure 5 as a solid line, and D has a value of −0.12 cm^{-1}. This anisotropy is not the single ion's anisotropy, and it has been observed in iron(III) (isotropic, S = 5/2) SMMs like Fe_8 and Fe_4 stars.[38] As Gatteschi and co-workers explain, the anisotropy arises in these cases from the spin−spin contribution and the axial-like anisotropy of the cluster. However, even though the ferromagnetic coupling seems intrinsic to Cu−Gd systems,[35c] as Wernsdorfer and Chibotaru point out, it is difficult to elucidate the origin of the small anisotropy of Cu−Gd complexes.[39]

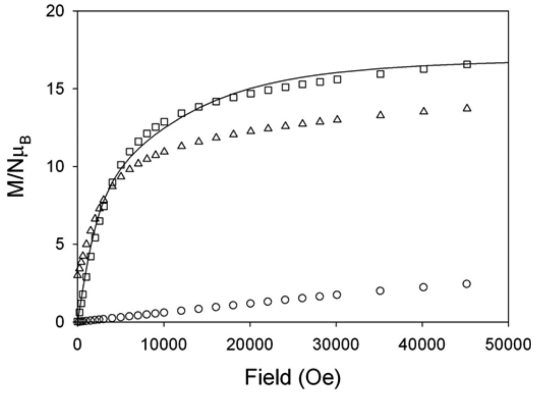

Figure 5. Magnetization vs field plots for **3** (circles), **4** (squares), and **5** (triangles) at 2 K. The solid line is the best fit to the experimental data for **4** (see text for fitting parameters).

In Table 3 are summarized the J values of magnetic interactions between Cu^{II} and Gd^{III} ions in a number of Cu^{II}−Gd^{III} compounds of different nuclearities and structural patterns as reported in recent times.[34,35] The values are largely ferromagnetic as expected, resulting from weak magnetic interactions between the participating metal centers.[35c] The largest J value reported so far is 10.1 cm^{-1}, while the smallest is around 0.11 cm^{-1}. An attempt has been made to correlate the J values with the Cu···Gd distances in such compounds using an exponential function: $-J = A \exp[Bd_{Gd\cdots Cu}]$ (where A and B are two constant terms, with J in cm^{-1} and $d_{Gd\cdots Cu}$ in Å), constructed purely on an empirical basis.[35a] One simple way to test the effectiveness of the above function is to examine the data collected from discrete binuclear Cu^{II}−Gd^{III} compounds.[35e,f] While in the compound $[L^1Cu^{II}Gd^{III}(NO_3)_3]\cdot Me_2CO$ Costes et al.[35e] reported a J value of 7.0(1) cm^{-1} for a Cu···Gd distance of 3.428(1) Å, Kahn et al.[35f] observed a J value of 1.42 cm^{-1} in another discrete binuclear compound, $[Salen(MeIm)Cu^{II}Gd^{III}(hfa)_3]$, in which the Cu···Gd distance [3.252(4) Å] is less than the former. This is contrary to what has been expected from the above equation, which is based on the premise that the nearer the Cu^{II} and Gd^{III} distance, the larger will be the exchange interaction in the molecule.[40] Another interesting structural difference between the above two dinuclear compounds concerns the GdO_2Cu bridging network, which is almost planar in the nitrato compound $[L^1Cu^{II}Gd^{III}(NO_3)_3]\cdot Me_2CO$ and bent along the O−O direction in $[Salen(MeIm)Cu^{II}Gd^{III}(hfa)_3]$ with a dihedral angle of 140.43° between the bridging O−Gd−O and O−Cu−O planes. As a result of this bending, the Cu−Gd magnetic interaction becomes poorer[41] in the latter compound, although the distance between the metal centers is shorter. Unfortunately, this correlation is valid for a strictly binuclear compound containing a pair of phenolato bridges.[42] Kahn et al.[35f] observed a remarkable change in the Cu^{II}−Gd^{III} exchange coupling in an apparently similar compound, $[Cu^{II}(salen)Gd^{III}(hfa)_3]_2$, with a dimeric structure where the binuclear $[Cu^{II}(salen)Gd^{III}(hfa)_3]$ units are oligomerized to form a dimeric unit due to the absence of an axial ligand (*N*-methylimidazole in the present case). The drastically reduced J_{Gd-Cu} = 0.4 cm^{-1} in this compound is believed to be due to the presence of strong intermolecular antiferromagnetic Cu^{II}−Cu^{II} interactions that make the interpretation more complicated.[35f] Thus, for polynuclear Cu^{II}−Gd^{III} compounds, interpretation of magnetic data becomes much more complicated due to the predominance of various other magnetic interactions including antiferromagnetic exchange between the copper centers, which lead mostly to a low-spin ground state (Table 3). One interesting aspect about the present series of compounds is their very unusual cage structure that isolates the three copper(II) centers from each other, leading to a high-spin ground state of 17/2 in **4**. However, the observed J_{Cu-Gd} value of 0.57 cm^{-1} in **4** is at the lower end of the observed range as found with Cu^{II}−Gd^{III} complexes of assorted nuclearities (Table 3). Deriving a clear magneto-structural correlation seems difficult at this stage for these compounds with multiple metal centers.

For compound **5**, the χT vs T plot is qualitatively similar to that observed with compound **4**. The χT product is almost flat in the 300 to 50 K temperature range and then increases with further decrease of temperature, indicating the Boltzman population of a ferromagnetically coupled spin ground state. This is confirmed by the magnetization vs field plots at 2 K for compounds **3** and **5**, also shown in Figure 5. For **3** the magnetization increases linearly with field, while for **5**

DOI: 10.1021/acs.inorgchem.5b01142
Inorg. Chem. 2015, 54, 9715−9726

Table 3. Exchange Coupling Constant Values J_{Cu-Gd} and J_{Cu-Cu} for Some Copper(II)−Gadolinium(III) Complexes of Assorted Nuclearities[a]

complex	nuclearity	ground state (S)	J_{Cu-Gd} (cm^{-1})	J_{Cu-Cu} (cm^{-1})	ref
$[L^1Cu^{II}Gd^{III}(NO_3)_3]\cdot Me_2CO$	$Cu^{II}Gd^{III}$	4	+7.0		35e
$[Salen(MeIm)Cu^{II}Gd^{III}(hfa)_3]$	$Cu^{II}Gd^{III}$	4	+1.42		35f
$[Cu^{II}(salen)Gd^{III}(hfa)_3]_2$	$Cu^{II}Gd^{III}$	4	+0.4		35f
$[(mosaldmtn)Cu^{II}Cl_2Gd^{III}(H_2O)_4]Cl\cdot 2H_2O$	$Cu^{II}Gd^{III}$	4	+10.1		42
$[(Cu^{II}hapen)_2Gd^{III}(H_2O)_3](ClO_4)_3\cdot 2Cu^{II}hapen$	$Cu^{II}_2Gd^{III}$	9/2	+5.32	−4.2	5
$[(Cu^{II}salen)_2Gd^{III}(H_2O)_3](ClO_4)_3\cdot 2Cusalen$	$Cu^{II}_2Gd^{III}$	9/2	+7.38	−12.23	5
$[Cu^{II}_3Gd^{III}(chp)_8(NO_3)(H_2O)]\cdot 0.5MeOH$	$Cu^{II}_3Gd^{III}$	4	+3.51, +0.11	−8.20, −12.52	35a
$[Cu^{II}_2Gd^{III}_2(mhp)_4(OMe)_2(NO_3)_4\text{-}(Hmph)_2MeOH)_2]$	$Cu^{II}_2Gd^{III}_2$		+0.15	−9.9	35a
$[(Cu^{II}L)_3Gd^{III}_2(\mu_3\text{-}O)_3H](ClO_4)$	$Cu^{II}_3Gd^{III}_2$	17/2	+0.57		this work
$[Cu^{II}_4Gd^{III}_2(hp)_8Cl_4(Hhp)_4(H_2O)_4]\cdot 2Cl.H_2O$	$Cu^{II}_4Gd^{III}_2$		+2.84, +0.55	−17.42	35a
$[Gd^{III}_2Cu^{II}_4(fsaaep)_4(NO_3)_6]\cdot 0.5(CH_3OH.H_2O)$	$Cu^{II}_4Gd^{III}_2$	9/2	+6.0	−3.13	35c
$Gd^{III}_4Cu^{II}_8L_8^2(\mu_2\text{-}H_2O)(\mu_3\text{-}OH)_8Cl_{10}(H_2O)_4]Cl_2\cdot 6MeCN$	$Cu^{II}_8Gd^{III}_4$		+0.5		35g
$[Cu^{II}_5Gd^{III}_4O_2(OMe)_4(teaH)_4(O_2CC\text{-}(CH_3)_3)_2(NO_3)_4]$	$Cu^{II}_5Gd^{III}_4$	31/2	−0.02, −0.09	0.10, −0.16	4f

[a] L^1 = 1,2′-bis((3-methoxysalicylidene)diamino)-2-methylpropane, MeIm = 1-methylimidazole, H_2salen = [*N*,*N*′-ethylenebis(salicylaldimine)], H_2mosaldmtn = 2,2′-[2,2-dimethyl-1,3-propanediylbis(nitrilomethylidyne)]bis(6-methoxyphenol), H_2apen = [*N*,*N*′-ethylenebis(*o*-hydroxyacetophenoneimine)], chp = anion of 6-chloro-2-pyridone, mhp = anion of 6-methyl-2-pyridone, hp = anion of 2-hydroxypyridine, H_2fsaaep = 3-(*N*-(2-pyridylethyl)formimidoyl)salicylic acid, HL^2 = 5,7-di-*tert*-butyl-2-methylenehydroxylbenzoxazole, $teaH_3$ = triethanolamine,

saturation is observed, as expected for a ferromagnetically coupled ground state.

Ac magnetic susceptibility data were collected for compounds **3**, **4**, and **5**. Of these, only **4**, the $Cu^{II}_3Gd^{III}_2$ complex, showed field-induced out-of-phase signals in the ac magnetic susceptibility plot vs T, as shown in Figure 6. If a dc field of

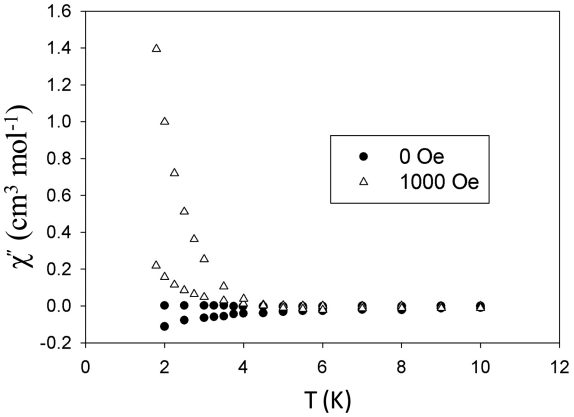

Figure 6. Ac magnetic susceptibility for **4** at 10 and 1000 Hz oscillating ac field and no applied dc field (plots with solid black circles) and 10 and 1000 Hz oscillating ac field and 1000 Oe applied dc field (plots with triangles).

1000 Oe is applied, the tail of an out-of-phase ac susceptibility plot that seems to be frequency dependent appears. This feature is in agreement with the switch-on of a possible SMM behavior when the dc field is applied. For a gadolinium compound, this observation is quite rare but not unprecendented.[39,43] Given the negative D value obtained for complex **4** and the spin ground state of 17/2, the energy barrier for **4** should be ca. $(S^2 - 1/4)|D| = 8\ cm^{-1}$. This is a very small barrier, and fast quantum tunneling would reduce it even more. The application of a dc field quenches quantum tunneling, and thus, the ac χ'' feature is shifted to higher temperatures, as observed here. Interestingly, compound **5** with an approximate spherical coordination environment around an ion like Tb^{III} does not give rise to a bistable state due to poor single-ion anisotropy, and thus no SMM behavior is observed[1a] in this compound.

PHOTOPHYSICAL STUDIES

Absorption Spectra. The absorption spectra of the free ligand and complexes **1**−**5** were recorded at 298 K in acetonitrile (Figure 7). The band at 285 nm for the free ligand

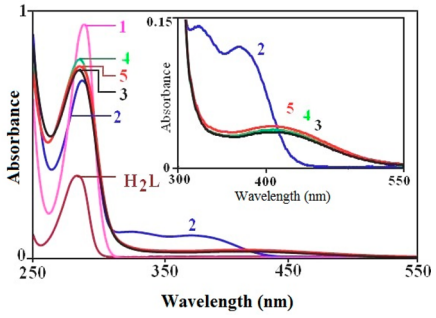

Figure 7. Absorption spectra in acetonitrile at 298 K (concentration = 60 μM in each case). Inset: Charge transfer bands are shown with change of scale for clarity.

is assigned as a $\pi \rightarrow \pi^*$ transition. All the complexes display the characteristic band centered at 285 nm, assigned due to localized $\pi \rightarrow \pi^*$ transition of the ligand. The extinction coefficient (ε) of this band for **1** is almost 3 times that of the free ligand since the complex contains three ligand moieties (Table 4). This band is slightly red-shifted (290 nm) in the case of complexes **1** and **2**. Complex **2** exhibits an additional broad band near 370 nm, and complexes **3**, **4**, and **5** exhibit an additional broad band near 415 nm (Figure 7). The position and the intensity of the broad bands are indicative of ligand-to-metal charge-transfer (^{1}LMCT) transitions.[13] The absorption maxima of the compounds and their molar extinction coefficients are presented in Table 4. The molar extinction coefficient values of complexes **2** to **5** are found to be lower compared to that of **1** for the band around 285 nm (Table 4). This could be attributed to the presence of an additional LMCT band in compounds **2**, **3**, **4**, and **5**. This LMCT band is

DOI: 10.1021/acs.inorgchem.5b01142
Inorg. Chem. 2015, 54, 9715−9726

Table 4. Absorption and Emission Data for the Free Ligand (H_2L) and the Complexes in Acetonitrile at 298 K

system	absorption maxima (nm), [ε] (M^{-1} cm^{-1})		fluorescence maxima (nm)	relative fluorescence quantum yield (Φ_D)[a] of ligand-based emission	singlet-state lifetimes monitoring the emission maxima (λ_{exc} = 290 nm) τ (ns)	χ^2	phosphorescence[b] maxima (nm) (λ_{exc} = 290 nm)	triplet state lifetimes (s) monitoring the emission maxima
free ligand	285 [6050][c]		318	1	1.00	1.08	435	0.9
1	290 [17 300]		337	0.40	0.45	0.98	430	0.8
2	289 [13 200]	370 [2275]	337	0.020	<0.15		430	0.4
3	286 [15 600]	415 [830]	337	0.025	<0.15		435	0.4
4	286 [15 900]	415 [840]	337	0.027	<0.15		435	0.4
5	286 [15 700]	415 [860]	337	0.026	<0.15		435	0.4

[a]Error in the measurement = ±5%. [b]Phosphorescence measurements were carried out in a rigid glassy matrix of 1:1 (v/v) mixed solvent of methanol and dichloromethane at 77 K. [c]For the measurement of the extinction coefficient (ε), sample concentration was 20 μM.

found to be more pronounced in **2** than those in **3**, **4**, and **5** (Figure 7).

Steady-State and Time-Resolved Emission Studies. The emission spectra of the free ligand and the complexes have been recorded in acetonitrile medium using λ_{exc} = 285 nm at 298 K. The free ligand shows an emission band peaking at 318 nm. When the complexes are excited at 290 nm, a broad emission centered at 337 nm (Figure 8, Table 4) is observed,

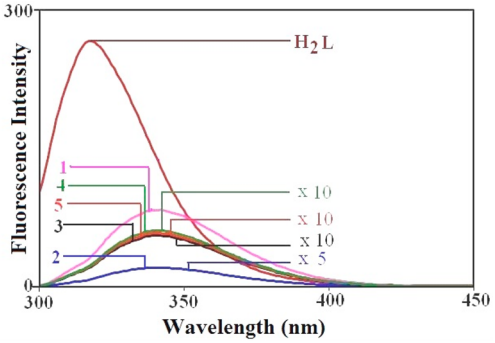

Figure 8. Fluorescence spectra in acetonitrile at 298 K. λ_{exc} = 285 nm for the ligand and the complexes **3**, **4**, and **5**; λ_{exc} = 290 nm for complexes **1** and **2**. Excitation band-pass = 10 nm and emission band-pass = 5 nm (optical densities of all the solutions were 0.2).

which can be attributed to the localized $\pi \rightarrow \pi^*$ transition of the ligand. The emission intensity has been found to be quenched in the complexes compared to that in the free ligand (Table 4). The quenching is found to be more prominent in the case of complexes **2** to **5**. The lifetime of the emission has been measured from the decay profile (Figure 9). The decays are found to fit with a single exponential (Table 4) having a χ^2 value close to 1. This is indicative of the presence of a single species in solution. The lifetime values observed for the ligand and complex **1** confirm the $\pi \rightarrow \pi^*$ nature of the emission. Since the emission of complexes **2** to **5** is largely quenched (Table 4), the singlet-state lifetimes are found to be less than 150 ps (beyond our detection limit with the λ_{exc} used for this purpose). The partial quenching of the emission of **1** compared to the free ligand could be due to the presence of Nd^{III} ions,

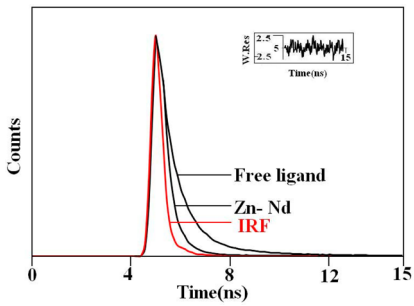

Figure 9. Fluorescence decay of the free ligand and complex **1** in acetonitrile at 298 K. λ_{exc} = 290 nm. Excitation band-pass = 5 nm and emission band-pass = 5 nm.

which enhances the intersystem crossing to the triplet state through the internal heavy atom effect. The distance of the Nd^{III} ions from the nearest ligand π-system as estimated from the crystal structure data is found to be around 4.5 Å, which is favorable for inducing an internal heavy atom effect.[44] The large quenching of the fluorescence in the Cu^{II} and Ni^{II} complexes is attributed to the paramagnetic nature of the transition metal ions involved[45] as well as to nonradiative decay of the $\pi-\pi^*$ singlet state to the LMCT state. The internal heavy atom effect due to the nearby Nd^{III} ions could be also partially responsible for quenching, as mentioned in the case of complex **1**. When complexes **2**−**5** are excited at their LMCT band, no corresponding emission is observed.

Low-Temperature Phosphorescence Spectra. In order to locate the lowest $\pi \rightarrow \pi^*$ triplet state in the ligand and in all the complexes, phosphorescence spectra are recorded in a rigid glassy matrix of 1:1 (v/v) mixed solvent of methanol and dichloromethane at 77 K. The free ligand and all the complexes exhibit a similar type of broad phosphorescence spectra peaking near 435 nm (Figure 10). The phosphorescence intensity is quenched in the complexes compared with that in the free ligand (Figure 10). The triplet-state populations in the case of complexes **2**, **3**, **4**, and **5** are found to be very low compared to that of the complex **1**. The lifetimes of the triplet state determined from the phosphorescence decay are summarized

DOI: 10.1021/acs.inorgchem.5b01142
Inorg. Chem. 2015, 54, 9715−9726

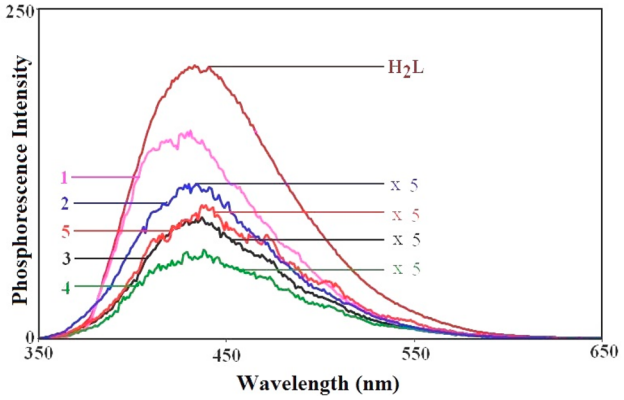

Figure 10. Phosphorescence spectra in a 1:1 (v/v) methanol–dichloromethane glassy matrix at 77 K. λ_{exc} = 285 nm for the ligand and complexes **3**, **4**, and **5**; λ_{exc} = 290 nm for complexes **1** and **2**. Excitation band-pass = 10 nm and emission band-pass = 5 nm.

in Table 4. The lifetime values are indicative of the $\pi \rightarrow \pi^*$ nature of the triplet state.[46]

Luminescence of Ln^{III}-3d Complexes. Among the reported complexes, only **1** exhibits lanthanide-based luminescence when excited in the $\pi \rightarrow \pi^*$ ligand band at 290 nm. The complex **1** shows NIR luminescence of Nd^{III} and exhibits characteristic peaks at 873 ($^4F_{3/2} \rightarrow {}^4I_{9/2}$), 1059 ($^4F_{3/2} \rightarrow {}^4I_{11/2}$), 1328 ($^4F_{3/2} \rightarrow {}^4I_{13/2}$), and 1775 nm ($^4F_{3/2} \rightarrow {}^4I_{15/2}$) (shown in Figure 11). The excitation spectrum monitoring the

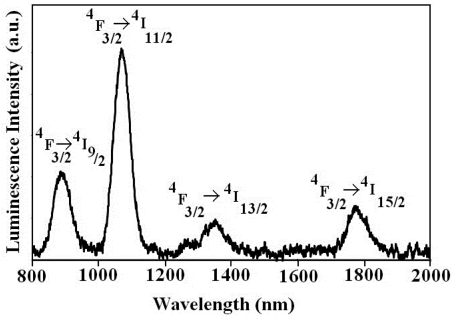

Figure 11. Luminescence spectrum of Nd^{III} in **1** in acetonitrile at 298 K; λ_{exc} = 290 nm. Excitation band-pass = 10 nm and emission band-pass = 10 nm (optical density of the solution was 0.2).

Nd^{III}-based transition ($^4F_{3/2} \rightarrow {}^4I_{11/2}$) at 1059 nm resembles the absorption spectrum of complex **1**. Direct f → f transitions of Nd^{III} ion are spin and parity forbidden. The efficient population of the emitting 4f excited states is achieved via intramolecular energy transfer from the ligand triplet state to the Nd^{III} f-excited state.[47] As the emitting state of Gd ^{III} resides above the singlet state of the ligand chromophore, there is no possibility of Gd^{III}-based emission in complex **4**. The absence of Ln^{III} emission in complexes **2**, **3**, and **5** at room temperature and also at 77 K in a glassy matrix could be attributed to (i) the lower population of the triplet state due to the paramagnetic nature of the associated 3d metal ions and (ii) the presence of an LMCT state in between the π–π^* singlet state and the lowest triplet state (Figure 12). The results imply that the CT state acts as a nonradiative channel and thus further inhibits the population of the Ln^{III} emitting state (Figure 12). The results clearly indicate that designing of d–f hybrid complexes exhibiting Ln^{III} luminescence needs a careful choice of

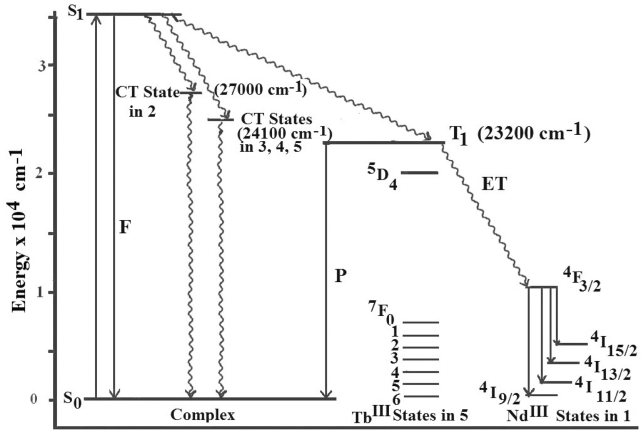

Figure 12. Energy level diagram of different states in the complexes. F and P stands for fluorescence and phosphorescence, respectively.

transition metal ion. The presence of a charge transfer singlet state in between the S_1 and T_1 states or close to the T_1 state could prevent energy transfer from the triplet state to the emitting state of Ln^{III}.

CONCLUSIONS

A new family of heterometal 3d–4f complexes (**1**–**5**) involving a phenol-based hexadentate ligand H_2L has been synthesized. The Cu_3Ln_2 (Ln = Nd^{III}, Gd^{III}, and Tb^{III}) compounds **3**–**5** show a change from antiferromagnetic coupling in **3** to ferromagnetic 3d–4f interactions in **4** and **5**. Simulation of the data for the $Cu^{II}{}_3Gd^{III}{}_2$ compound **4** provides ferromagnetic Cu–Gd (J_1 = 0.57 cm^{-1}) and Gd–Gd exchange constants (J_2 = 0.14 cm^{-1}) and a high-spin ground state of S_T = 17/2. Compound **4** displays a field-induced out-of-phase signal in the ac susceptibility measurement, indicative of slow relaxation of magnetization, and is a new, rare example of Cu–Gd SMM. This is possibly due to an interesting cage structure of the molecule, providing the opportunity to segregate the Cu^{II} centers from one another. This leads to a high-spin ground state that probably helps in displaying an SMM character. Thus, compound **4** turns out to be an interesting switchable material in which SMM behavior can be switched on by an applied dc field. Out of the three $M^{II}{}_3Nd^{III}{}_2$ (M = Zn^{II}, Cu^{II}, and Ni^{II}) complexes, only the Zn^{II} analogue (**1**) displays an NIR luminescence due to the $^4F_{3/2} \rightarrow {}^4I_{11/2}$ transition when excited at 290 nm. The Cu_3Tb_2 complex also failed to display Tb^{III}-based emission. The paramagnetic nature of the transition metal ions could quench the fluorescence and thus lowers the population of the triplet state. Furthermore, the presence of an LMCT singlet state in between the π–π^* S1 and T_1 states could prevent energy transfer from the triplet state to the emitting state of Nd^{III}/Tb^{III}.

ASSOCIATED CONTENT

Supporting Information

The Supporting Information is available free of charge on the ACS Publications website at DOI: 10.1021/acs.inorgchem.5b01142.

Perspective views of the molecular structures of **1**, **2**, **4**, and **5** (Figures S1–S4) (PDF)

X-ray crystallographic files in CIF format for compound **1** (CIF)

DOI: 10.1021/acs.inorgchem.5b01142
Inorg. Chem. 2015, 54, 9715–9726

X-ray crystallographic files in CIF format for compound **2** (CIF)
X-ray crystallographic files in CIF format for compound **3** (CIF)
X-ray crystallographic files in CIF format for compound **4** (CIF)
X-ray crystallographic files in CIF format for compound **5** (CIF)

AUTHOR INFORMATION

Corresponding Author

*E-mail: icmc@iacs.res.in.

Notes

The authors declare no competing financial interest.

ACKNOWLEDGMENTS

This paper is dedicated to Professor Ajoy Kumar Ray on the occasion of his 65th birthday. The work was supported by the Council of Scientific and Industrial Research (CSIR), New Delhi (No. 01(2557)/12/EMR-II). Three of the authors, M.M., M.C.M., and S.K., also thank the CSIR for the award of research fellowships. The single-crystal X-ray diffraction data were recorded on an instrument supported by DST, New Delhi, as a National Facility at IACS under the IRHPA program. S.G. gratefully acknowledges DST (SB/S1/PC-003/2013) and CSIR (No. 21(0871)/11/EMR-II) for financially supporting this work. S.K.S. acknowledges CSIR for an SRF fellowship (No. 08/155(0039)/2009-EMR-I). E.C.S. acknowledges the financial support from the Spanish Government, (Grant CTQ2012-32247).

REFERENCES

(1) (a) Rinehart, J. D.; Long, J. R. *Chem. Sci.* **2011**, *2*, 2078. (b) Sorace, L.; Benelli, C.; Gatteschi, D. *Chem. Soc. Rev.* **2012**, *42*, 3278. (c) Luzon, J.; Sessoli, R. *Dalton Trans.* **2012**, *41*, 13556.

(2) (a) Clemente-Juan, J. M.; Coronado, E.; Gaita-Ariño, A. *Chem. Soc. Rev.* **2012**, *41*, 7464. (b) Woodruff, D. N.; Winpenny, R. E. P.; Layfield, R. A. *Chem. Rev.* **2013**, *113*, 5110.

(3) Gatteschi, D.; Sessoli, R.; Villain, J. *Molecular Nanomagnets*; Oxford University Press: Oxford, U.K., 2006.

(4) (a) Evangelisti, M.; Brechin, E. K. *Dalton Trans.* **2010**, *39*, 4672. (b) Evangelisti, M.; Roubeau, O.; Palacios, E.; Camón, A.; Hooper, T. N.; Brechin, E. K.; Alonso, J. J. *Angew. Chem., Int. Ed.* **2011**, *50*, 6606. (c) Hooper, T. N.; Schnack, J.; Piligkos, S.; Evangelisti, M.; Brechin, E. K. *Angew. Chem., Int. Ed.* **2012**, *51*, 4633. (d) Guo, F. S.; Chen, Y. C.; Mao, L. L.; Lin, W. Q.; Leng, J. D.; Tarasenko, R.; Orendac, M.; Prokleska, J.; Sechovsky, V.; Tong, M. L. *Chem. - Eur. J.* **2013**, *19*, 14876. (e) Lorusso, G.; Sharples, J. W.; Palacios, E.; Roubeau, O.; Brechin, E. K.; Sessoli, R.; Rossin, A.; Tuna, F.; Mclnnes, E. J. L.; Collison, D.; Evangelisti, M. *Adv. Mater.* **2013**, *25*, 4653. (f) Rajeshkumar, T.; Annadata, H. V.; Evangelisti, M.; Langley, S. K.; Chilton, N. F.; Murray, K. S.; Rajaraman, G. *Inorg. Chem.* **2015**, *54*, 1661.

(5) Bencini, A.; Benelli, C.; Caneschi, A.; Carlin, R. L.; Dei, A.; Gatteschi, D. *J. Am. Chem. Soc.* **1985**, *107*, 8128.

(6) (a) Zaleski, C. M.; Kampf, J. W.; Mallah, T.; Kirk, M. L.; Pecoraro, V. L. *Inorg. Chem.* **2007**, *46*, 1954. (b) Zaleski, C. M.; Depperman, E. C.; Kampf, J. W.; Kirk, M. L.; Pecoraro, V. L. *Angew. Chem., Int. Ed.* **2004**, *43*, 3912. (c) Stamatatos, T. C.; Teat, S. J.; Wernsdorfer, W.; Christou, G. *Angew. Chem., Int. Ed.* **2009**, *48*, 521. (d) Mereacre, V.; Ako, A. M.; Clerac, R.; Wernsdorfer, W.; Hewitt, I. J.; Anson, C. E.; Powell, A. K. *Chem. - Eur. J.* **2008**, *14*, 3577. (e) Mishra, A.; Wernsdorfer, W.; Parsons, S.; Christou, G.; Brechin, E. K. *Chem. Commun.* **2005**, 2086. (f) Mishra, A.; Tasiopoulos, A. J.; Wernsdorfer, W.; Moushi, E. E.; Moulton, B.; Zaworotko, M. J.; Abboud, K. A.; Christou, G. *Inorg. Chem.* **2008**, *47*, 4832. (g) Akhtar, M. N.; Mereacre, V.; Novitchi, G.; Tuchagues, J.-P.; Anson, C. E.; Powell, A. K. *Chem. - Eur. J.* **2009**, *15*, 7278. (h) Abbas, G.; Lan, Y.; Mereacre, V.; Wernsdorfer, W.; Clerac, R.; Buth, G.; Sougrati, M. T.; Grandjean, F.; Long, G. J.; Anson, C. E.; Powell, A. K. *Inorg. Chem.* **2009**, *48*, 9345. (i) Ferbinteanu, M.; Kajiwara, T.; Choi, K. Y.; Nojiri, H.; Nakamoto, A.; Kojima, N.; Cimpoesu, F.; Fujimura, Y.; Takaishi, S.; Yamashita, M. *J. Am. Chem. Soc.* **2006**, *128*, 9008. (j) Pineda, E. M.; Tuna, F.; Pritchard, R. G.; Regan, A. C.; Winpenny, R. E. P.; McInnes, E. J. L. *Chem. Commun.* **2013**, *49*, 3522. (k) Zheng, Y.-Z.; Evangelisti, M.; Tuna, F.; Winpenny, R. E. P. *J. Am. Chem. Soc.* **2012**, *134*, 1057. (l) Zheng, Y.-Z.; Evangelisti, M.; Winpenny, R. E. P. *Chem. Sci.* **2011**, *2*, 99. (m) Chandrasekhar, V.; Pandian, B. M.; Vittal, J. J.; Clerac, R. *Inorg. Chem.* **2009**, *48*, 1148. (n) Yamaguchi, T.; Costes, J.-P.; Kishima, Y.; Kojima, M.; Sunatsuki, Y.; Brefuel, N.; Tuchagues, J.-P.; Vendier, L.; Wernsdorfer, W. *Inorg. Chem.* **2010**, *49*, 9125. (o) Zou, L.-F.; Zhao, L.; Guo, Y.-N.; Yu, G.-M.; Guo, Y.; Tang, J.; Li, Y.-H. *Chem. Commun.* **2011**, *47*, 8659. (p) Gomez, V.; Vendier, L.; Corbella, M.; Costes, J.-P. *Inorg. Chem.* **2012**, *51*, 6396. (q) Mondal, K. C.; Sundt, A.; Lan, Y.; Kostakis, G. E.; Waldmann, O.; Ungur, L.; Chibotaru, L. F.; Anson, C. E.; Powell, A. K. *Angew. Chem., Int. Ed.* **2012**, *51*, 7550. (r) Sopasis, G. J.; Orfanoudaki, M.; Zarmpas, P.; Philippidis, A.; Siczek, M.; Lis, T.; O'Brien, J. R.; Milios, C. J. *Inorg. Chem.* **2012**, *51*, 1170. (s) Towatari, M.; Nishi, K.; Fujinami, T.; Matsumoto, N.; Sunatsuki, Y.; Kojima, M.; Mochida, N.; Ishida, T.; Re, N.; Mrozinski, J. *Inorg. Chem.* **2013**, *52*, 6160.

(7) (a) Novitchi, G.; Wernsdorfer, W.; Chibotaru, L. F.; Costes, J. P.; Anson, C. E.; Powell, A. K. *Angew. Chem., Int. Ed.* **2009**, *48*, 1614. (b) Kajiwara, T.; Nakano, M.; Takaishi, S.; Yamashita, M. *Inorg. Chem.* **2008**, *47*, 8604. (c) Costes, J.-P.; Dahan, F.; Wernsdorfer, W. *Inorg. Chem.* **2006**, *45*, 5. (d) Osa, S.; Kido, T.; Matsumoto, N.; Re, N.; Pochaba, A.; Mrozinski, J. *J. Am. Chem. Soc.* **2004**, *126*, 420. (e) Aronica, C.; Pilet, G.; Chastanet, G.; Wernsdorfer, W.; Jacquot, J. F.; Luneau, D. *Angew. Chem., Int. Ed.* **2006**, *45*, 4659. (f) Aronica, C.; Chastanet, G.; Pilet, G.; Le Guennic, B.; Robert, V.; Wernsdorfer, W.; Luneau, D. *Inorg. Chem.* **2007**, *46*, 6108. (g) Okazawa, A.; Nogami, T.; Nojiri, H.; Ishida, T. *Chem. Mater.* **2008**, *20*, 3110. (h) Okazawa, A.; Nogami, T.; Nojiri, H.; Ishida, T. *Inorg. Chem.* **2008**, *47*, 9763. (i) Okazawa, A.; Nogami, T.; Nojiri, H.; Ishida, T. *Inorg. Chem.* **2009**, *48*, 3292. (j) Iasco, O.; Novitchi, G.; Jeanneau, E.; Wernsdorfer, W.; Luneau, D. *Inorg. Chem.* **2013**, *52*, 8723. (k) Chaudhari, A. K.; Joarder, B.; Rivière, E.; Rogez, G.; Ghosh, S. K. *Inorg. Chem.* **2012**, *51*, 9159. (l) Sopasis, G. J.; Canaj, A. B.; Philippidis, A.; Siczek, M.; Lis, T.; O'Brien, J. R.; Antonakis, M. M.; Pergantis, S. P.; Milios, C. J. *Inorg. Chem.* **2012**, *51*, 5911.

(8) (a) Wernsdorfer, W.; Aliaga-Alcade, N.; Hendrickson, D. N.; Christou, G. *Nature* **2002**, *416*, 406. (b) Leuenberger, M. N.; Loss, D. *Nature* **2001**, *410*, 789. (c) Ritter, S. K. *Chem. Eng. News* **2004**, *82*, 29. (d) Sessoli, R.; Gatteschi, D.; Caneschi, A.; Novak, M. *Nature* **1993**, *365*, 141. (e) Inglis, R.; Jones, L. F.; Karotsis, G.; Collins, A.; Parsons, S.; Perlepes, S. P.; Wernsdorfer, W.; Brechin, E. K. *Chem. Commun.* **2008**, 5924. (f) Maheswaran, S.; Chastanet, G.; Teat, S. J.; Mallah, T.; Sessoli, R.; Wernsdorfer, W.; Winpenny, R. E. P. *Angew. Chem., Int. Ed.* **2005**, *44*, 5044. (g) Binnemans, K.; Galyametdinov, Y. G.; Van Deun, R.; Bruce, D. W.; Collinson, S. R.; Polishchuk, A. P.; Bikchantaev, I.; Haase, W.; Prosvirin, A. V.; Tinchurina, L.; Litvinov, U.; Gubajdullin, A.; Rakhmatullin, A.; Uytterhoeven, K.; Van Meervelt, L. *J. Am. Chem. Soc.* **2000**, *122*, 4335. (h) Gschneidner, K. A., Jr.; Pecharsky, V. K. L. *J. Appl. Phys.* **1999**, *85*, 5365.

(9) (a) Reisfeld, R.; Jørgensen, C. K. *Lasers and Excited States of Rare Earths*; Springer: Heidelberg, 1977. (b) Gan, F. *Laser Materials*; World Scientific: Singapore, 1995; p 209. (c) Faulkner, S.; Matthews, J. L. *Comprehensive Coordination Chemistry, Application of Coordination Complexes*, 2nd ed.; Ward, M. D., Ed.; Elsevier: Oxford, UK, 2004; p 913. (d) *The Chemistry of Contrast Agents in Medical Magnetic Resonance Imaging*; Merbach, A. E., Toth, E., Eds.; John Wiley: London, 2001. (e) Charbonnière, L.; Ziessel, R.; Guardigli, M.; Roda, A.; Sabbatini, N.; Cesario, M. *J. Am. Chem. Soc.* **2001**, *123*, 2436 and

DOI: 10.1021/acs.inorgchem.5b01142
Inorg. Chem. 2015, 54, 9715−9726

references therein. (f) Faulkner, S.; Pope, S. J. A.; Burton-Pye, B. P. *Appl. Spectrosc. Rev.* **2005**, *40*, 1.
(10) (a) Cui, Y.; Yue, Y.; Qian, G.; Chen, B. *Chem. Rev.* **2012**, *112*, 1126. (b) Binnemans, K. *Chem. Rev.* **2009**, *109*, 4283. (c) Bünzli, J.-C. G.; Piguet, C. *Chem. Rev.* **2002**, *102*, 1897. (d) Bünzli, J.-C. G.; Chauvin, A.-S.; Kim, H. K.; Deiters, E.; Eliseeva, S. V. *Coord. Chem. Rev.* **2010**, *254*, 2623. (e) Shavaleev, N. M.; Moorcraft, L. P.; Pope, S. J. A.; Bell, Z. R.; Faulkner, S.; Ward, M. D. *Chem. - Eur. J.* **2003**, *9*, 5283. (f) Bennett, S. D.; Pope, S. J. A.; Ward, B. D. *Chem. Commun.* **2013**, *49*, 6072. (g) Shavaleev, N. M.; Accorsi, G.; Virgili, D.; Bell, Z. R.; Lazarides, T.; Calogero, G.; Armaroli, N.; Ward, M. D. *Inorg. Chem.* **2005**, *44*, 61. (h) Comby, S.; Imbert, D.; Chauvin, A.-S.; Bünzli, J.-C. G. *Inorg. Chem.* **2006**, *45*, 732. (i) Wong, W.-K.; Yang, X.; Jones, R. A.; Rivers, J. H.; Lynch, V.; Lo, W.-K.; Xiao, D.; Oye, M. M.; Holmes, A. L. *Inorg. Chem.* **2006**, *45*, 4340. (j) Baca, S. G.; Pope, S. J. A.; Adams, H.; Ward, M. D. *Inorg. Chem.* **2008**, *47*, 3736. (k) Pasatoiu, T. D.; Tiseanu, C.; Madalan, A. M.; Jurca, B.; Duhayon, C.; Sutter, J. P.; Andruh, M. *Inorg. Chem.* **2011**, *50*, 5879.
(11) Nonat, A.; Imbert, D.; Pecaut, J.; Giraud, M.; Mazzanti, M. *Inorg. Chem.* **2009**, *48*, 4207.
(12) (a) Silver, J. In *Comprehensive Coordination Chemistry*, 2nd ed.; Ward, M. D., Ed.; Elsevier: Oxford, U.K., 2004; Vol. 9 p 689. (b) Kido, J.; Okamoto, Y. *Chem. Rev.* **2002**, *102*, 2357. (c) Sabbatini, N.; Guardigli, M.; Lehn, J.-M. *Coord. Chem. Rev.* **1993**, *123*, 201.
(13) (a) Tojal, J. G.; Orad, A. G.; Serra, J. L.; Pizarro, J. L.; Lezama, L.; Arriortua, M. I.; Rojo, T. *J. Inorg. Biochem.* **1999**, *75*, 45. (b) Casella, L.; Gullotti, M.; Pallanza, G.; Buga, M. *Biol. Met.* **1990**, *3*, 137. (c) Lewis, D. J.; Deshmukh, P.; Tedstone, A. A.; Tuna, F.; O'Brien, P. *Chem. Commun.* **2014**, *50*, 13334. (d) Carrasco, R.; Cano, J.; Ottenwaelder, X.; Aukauloo, A.; Journaux, Y.; García, R. R. *Dalton Trans.* **2005**, 2527. (e) Sarı, N.; Şahin, S. Ç.; Öğütcü, H.; Dede, Y.; Yalcin, S.; Altundas, A.; Doğanay, K. *Spectrochim. Acta, Part A* **2013**, *106*, 60.
(14) Abtab, S. M. T.; Majee, M. C.; Maity, M.; Titiš, J.; Boča, R.; Chaudhury, M. *Inorg. Chem.* **2014**, *53*, 1295.
(15) Abtab, S. M. T.; Audhya, A.; Kundu, N.; Samanta, S. K.; Saha Sardar, P.; Butcher, R. J.; Ghosh, S.; Chaudhury, M. *Dalton Trans.* **2013**, *42*, 1848.
(16) Abtab, S. M. T.; Maity, M.; Bhattacharya, K.; Sañudo, E. C.; Chaudhury, M. *Inorg. Chem.* **2012**, *51*, 10211.
(17) See for example: (a) Mondal, K. C.; Kostakis, G. E.; Lan, Y.; Wernsdorfer, W.; Anson, C. E.; Powell, A. K. *Inorg. Chem.* **2011**, *50*, 11604. (b) Goura, J.; Guillaume, R.; Rivière, E.; Chandrasekhar, V. *Inorg. Chem.* **2014**, *53*, 7815. (c) Andruh, M.; Costes, J. P.; Diaz, C.; Gao, S. *Inorg. Chem.* **2009**, *48*, 3342. (d) Jana, A.; Majumder, S.; Carrella, L.; Nayak, M.; Weyhermueller, T.; Dutta, S.; Schollmeyer, D.; Rentschler, E.; Koner, R.; Mohanta, S. *Inorg. Chem.* **2010**, *49*, 9012. (e) Palacios, M. A.; Padilla, S. T.; Ruiz, J.; Herrera, J. M.; Pope, S. J. A.; Brechin, E. K.; Colacio, E. *Inorg. Chem.* **2014**, *53*, 1465. (f) Hanninen, M. M.; Valivaara, J.; Mota, A. J.; Colacio, E.; Lloret, F.; Sillanpaä, R. *Inorg. Chem.* **2013**, *52*, 2228. (g) Hänninen, M. M.; Mota, A. J.; Aravena, D.; Ruiz, E.; Sillanpää, R.; Camón, A.; Evangelisti, M.; Colacio, E. *Chem. - Eur. J.* **2014**, *20*, 8410.
(18) Perrin, D. D.; Armarego, W. L. F.; Perrin, D. R. *Purification of Laboratory Chemicals*, 2nd ed.; Pergamon: Oxford, England, 1980.
(19) Robinson, W. R. *J. Chem. Educ.* **1985**, *62*, 1001.
(20) *SADABS*, version 2.03; Bruker AXS Inc.: Madison, WI, 2002.
(21) Sheldrick, G. M. *Acta Crystallogr., Sect. A: Found. Crystallogr.* **1990**, *46A*, 467.
(22) Sheldrick, G. M. *SHELXL-2013*; University of Gottingen: Gottingen, Germany, 2013.
(23) *SAINT*, version 6.02; Bruker AXS Inc.: Madison, WI, 2002.
(24) *DIAMOND, Visual Crystal Structure Information System*, version 3.1; Crystal Impact: Bonn, Germany, 2004.
(25) Bevington, P. R. *Data Reduction and Error Analysis for the Physical Sciences*; McGraw Hill: New York, 1969; pp 235−237.
(26) *FELIX 32*, Operation Manual, Version 1.1; Photon Technology International, Inc.: Birmingham, NJ, 2003.
(27) *FELIX GX*, Operation Manual, Version 2.0.1; Photon Technology International, Inc.: Birmingham, NJ, 2003.
(28) Nakamoto, K. *Infrared and Raman Spectra of Inorganic and Coordination Compounds*, 3rd ed.; Wiley-Interscience: New York, 1978.
(29) Addison, A. W.; Rao, T. N.; Reedijk, J.; van Rijn, J.; Verschoor, G. C. *J. Chem. Soc., Dalton Trans.* **1984**, 1349.
(30) Costes, J. − P.; Duhayon, C.; Vendier, L. *Inorg. Chem.* **2014**, *53*, 2181.
(31) (a) Kahn, O. *Molecular Magnetism*; VCH Publ. Inc.: New York, 1993. (b) Millar, J. S.; Drillon, M. *Magnetism: Molecule to Materials*; Wiley-VCH: Weinheim, 2005; Vol. *V*.
(32) Liu, J. L.; Yuan, K.; Leng, J. D.; Ungur, L.; Wernsdorfer, W.; Guo, F. S.; Chibotaru, L. F.; Tong, M. L. *Inorg. Chem.* **2012**, *51*, 8538.
(33) Rosado Piquer, L.; Sañudo, E. C. *Dalton Trans.* **2015**, *44*, 8771.
(34) Kahn, M. L.; Mathonière, C.; Kahn, O. *Inorg. Chem.* **1999**, *38*, 3692.
(35) See for example: (a) Benelli, C.; Blake, A. J.; Milne, P. E. Y.; Rawson, J. M.; Winpenny, R. E. P. *Chem. - Eur. J.* **1995**, *1*, 614. (b) Bencini, A.; Benelli, C.; Caneschi, A.; Dei, A.; Gatteschi, D. *Inorg. Chem.* **1986**, *25*, 572. (c) Andruh, M.; Ramade, I.; Codjovi, E.; Guillou, O.; Kahn, O.; Trombe, J. C. *J. Am. Chem. Soc.* **1993**, *115*, 1822. (d) Costes, J.-P.; Dahan, F.; Dupuis, A.; Laurent, J.-P. *Inorg. Chem.* **1997**, *36*, 3429. (e) Costes, J. P.; Dahan, F.; Dupuis, A.; Laurent, J. P. *Inorg. Chem.* **1996**, *35*, 2400. (f) Ramade, I.; Kahn, O.; Jeannin, Y.; Robert, F. *Inorg. Chem.* **1997**, *36*, 930. (g) Iasco, O.; Novitchi, G.; Jeanneau, E.; Wernsdorfer, W.; Luneau, D. *Inorg. Chem.* **2011**, *50*, 7373.
(36) (a) Costes, J.-P.; Dahan, F.; Dupuis, A. *Inorg. Chem.* **2000**, *39*, 5994. (b) Langley, S. K.; Ungur, L.; Chilton, N. F.; Moubaraki, B.; Chibotaru, L. F.; Murray, K. S. *Chem. - Eur. J.* **2011**, *17*, 9209. (c) Sakamoto, M.; Manseki, K.; Ōkawa, H. *Coord. Chem. Rev.* **2001**, *219*−*221*, 379.
(37) Chilton, N. F.; Anderson, R. P.; Turner, L. D.; Soncini, A.; Murray, K. S. *J. Comput. Chem.* **2013**, *34*, 1164.
(38) Gatteschi, D.; Sessoli, R.; Cornia, A. *Chem. Commun.* **2000**, 725.
(39) Borta, A.; Jeanneau, E.; Chumakov, Y.; Luneau, D.; Ungur, L.; Chibotaru, L. F.; Wernsdorfer, W. *New J. Chem.* **2011**, *35*, 1270.
(40) Winpenny, R. E. P. *Chem. Soc. Rev.* **1998**, *27*, 447.
(41) (a) Charlot, M. F.; Jeannin, S.; Jeannin, Y.; Kahn, O.; Lucrèce-Abaul, J.; Martin-Frère, J. *Inorg. Chem.* **1979**, *18*, 1675. (b) Charlot, M. F.; Kahn, O.; Jeannin, S.; Jeannin, Y. *Inorg. Chem.* **1980**, *19*, 1410. (c) Journaux, Y.; Kahn, O.; Morgenstern-Badarau, I.; Galy, J.; Jaud, J.; Bencini, A.; Gatteschi, D. *J. Am. Chem. Soc.* **1985**, *107*, 6305.
(42) Costes, J.-P.; Dahan, F.; Dupuis, A. *Inorg. Chem.* **2000**, *39*, 165.
(43) (a) Yamaguchi, T.; Costes, J.-P.; Kishima, Y.; Kojima, M.; Sunatsuki, Y.; Bréfuel, N.; Tuchagues, J.-P.; Vendier, L.; Wernsdorfer, W. *Inorg. Chem.* **2010**, *49*, 9125. (b) Chandrasekhar, V.; Murugesu Pandian, B.; Azhakar, R.; Vittal, J. J.; Clérac, R. *Inorg. Chem.* **2007**, *46*, 5140.
(44) (a) Bhattacharya, S.; Basu Roy, M.; Ghosh, S. *Chem. Phys.* **2004**, *300*, 295. (b) Ghosh, S.; Petrin, M.; Maki, A. H.; Sousa, L. R. *J. Chem. Phys.* **1987**, *87*, 4315.
(45) (a) Volchkov, V. V.; Ivanov, V. L.; Uzhinov, B. M. *J. Fluoresc.* **2010**, *20*, 299. (b) Homan, R.; Eisenberg, M. *Biochim. Biophys. Acta, Biomembr.* **1985**, *812*, 485. (c) Chang, J. H.; Choi, Y. M.; Shin, Y.-K. *Bull. Korean Chem. Soc.* **2001**, *22*, 527. (d) Kemlo, J. A.; Shepard, T. M. *Chem. Phys. Lett.* **1977**, *47*, 158. (e) Varnes, A. W.; Dodson, R. B.; Wehry, E. L. *J. Am. Chem. Soc.* **1972**, *94*, 946.
(46) Angulo, G.; Grilj, J.; Vauthey, E.; Andrés, L. S.; Pons, Ó. R.; Jacques, P. *ChemPhysChem* **2010**, *11*, 480.
(47) Barry, D. E.; Kitchen, J. A.; Albrecht, M.; Faulkner, S.; Gunnlaugsson, T. *Langmuir* **2013**, *29*, 11506.

DOI: 10.1021/acs.inorgchem.5b01142
Inorg. Chem. 2015, 54, 9715−9726